NATIONAL GEOPHYSICAL DATA CENTER
PRESENTS
SCIENTIFIC AND EDUCATIONAL SLIDE SETS

Unless otherwise noted, each set contains 20 color slides.

Aurora Australis (Southern Lights)

Twenty spectacular slides taken by David Miller from Kangaroo Island, Southern Australia during intense solar activity. These wonderful pictures show breathtaking colors and forms of auroras, framed against landscapes and a backdrop of stars.

Aurora and Other Lights Viewed from Space

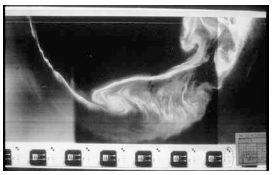

Fifty-two slides of Aurora and other nocturnal lights viewed from space. 35mm imagery from the Defense Meteorological Satellite Program taken between 1973 and 1977. B&W

Behavior of Columns during Earthquakes

Column failure is a primary cause of structure collapse in earthquakes. This set illustrates a variety of types of column failure, including: inadequate beam-to-column and slab-to-column connection, over stressed columns, and columns of unequal length.

Cape Mendocino, California Earthquakes, April 25 & 26, 1992

Illustrations of the effects and damage of a moderately large earthquake (7.1) and aftershocks (6.6 & 6.7) on the sparsely populated, southwestern Humboldt County, California.

Coral Paleoclimatology

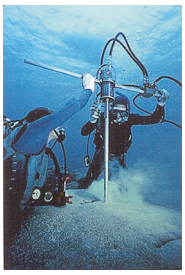

Professional underwater photography of corals and the coring process. Illustration of climate reconstructions, including El Niño, presenting data obtained from geochemical analysis of coral samples.

Coral Paleoclimatology, High School Version

Secondary school version of Coral Paleoclimatology with emphasis on tropical ecosystems and less technical coverage of geochemistry. 24 slides

Crater Peak (Mt. Spurr), Alaska: Eruptions of 1992

This set follows the story of Crater Peak activity from June through October 1992. It depicts precursors, the eruptions, and effects on the environment and the population.

Düzce, Turkey Earthquake, November 12, 1999

These slides show damage from the second major earthquake (7.2) to hit Kocaeli province, in northwestern Turkey, in four months. The epicenter is on the eastern fringe of the area affected by the Izmit earthquake that occurred in August and killed more than 17,000 people.

Earthquake Damage – General

This set provides an overview and summary of effects caused by eleven earthquakes in eight countries. The images depict surface faulting, landslides, soil liquefaction, and structural damage.

Earthquake Damage in Mexico City, Mexico, September 19, 1985

Pictures of different types of damaged buildings and the major kinds of structural failure that occurred in Mexico City, at a 350 km distance from the epicenter of a magnitude 8.1 earthquake. Effect of subsoils on earthshaking and building damage, is emphasized.

Earthquake Damage in San Francisco, California, April 18, 1906

The 1906 San Francisco magnitude 8.3 earthquake was the largest 20th century event to occur in the conterminous United States. This set includes a panoramic view of San Francisco in flames a few hours after the earthquake, damage scenes from the area, and other historic photographs. B&W

Earthquake Damage to Schools

The set graphically illustrates the potential danger that major earthquakes pose to school structures and occupants. It includes pictures from 1886 to 1988 of nine destructive earthquakes in the U.S. and eight earthquakes that occurred in foreign countries. B&W/Color

Earthquake Damage to Transportation Systems

A serious result of large-magnitude earthquakes is the disruption of transportation systems, inhibiting emergency response. These slides depict damage to transportation systems sorted by cause such as ground failure, faulting, vibration damage, and tsunamis. B&W/Color

Earthquake Damage, Armenian SSR, December 7, 1988

This magnitude 6.9 earthquake in northwestern Armenia was followed minutes later by a magnitude 5.8 aftershock. These photographs show damage in and around the devastated cities of Spitak and Leninakan.

Earthquake Damage, Northern Iran, June 21, 1990

This unusually destructive magnitude 7.7 earthquake appeared to be multiple earthquakes occurring in rapid succession. This set depicts damage resulting from intensive ground motion and soil liquefaction, acting on unreinforced masonry, steel structures, and concrete buildings.

Earthquakes in Central California, 1980-1984

Slides showing earthquake damage from the following central California events: Livermore, 1980, Coalinga, 1983, and Morgan Hill, 1984. All of these earthquakes were greater than magnitude 5.8 or caused estimated damage in excess of 8 million dollars.

Earthquakes in Southern California

These slides show damage from the following Southern California earthquakes: Imperial Valley, 1979, Westmorland, 1981, Palm Springs, 1986, and Whittier, 1987. All of these earthquakes were greater than magnitude 5.9 or caused estimated damage in excess of one million dollars.

El Quindio, Colombia Earthquake, January 25, 1999

The El Quindio earthquake was one of the most destructive in Colombia in recent years because of three factors: the presence of faults, infill walls, and "soft" soils. This set depicts damage from the January event.

Environmental Hazards and Mud Volcanoes in Romania

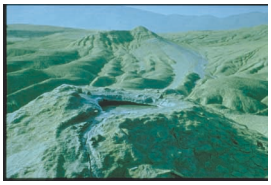

Romanian researchers have a long tradition of studying the natural hazards, which disrupt their society. These slides show examples of landslides, rockfalls, sheet erosion, and mudflows.

Erosional Landforms

Dramatic views of erosional landforms sculpted by rivers, glaciers, and waves. Many of the locales include U.S. National Parks and Monuments.

Eruption of Mount St. Helens, May 18, 1980

The Mount St. Helens eruption has afforded geologists a unique opportunity to learn about volcanoes. These slides not only include pictures of the eruption, but pre-eruption activity and post-eruption geomorphology.

Faults

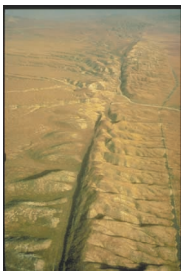

Faults reveal information about crustal movements and earthquake size and recurrence intervals. This set describes fault types and mechanisms and their effects on natural and manmade features.

Fire *vs*. Water: The Erosional & Depositional Geology of Hawaiian Islands

The opposing forces of volcanism and erosion shape Hawaii's dramatic geology. This set shows constructional volcanic features and their subsequent erosion.

Great Alaska Earthquake, Prince William Sound, March 28, 1964

The Prince William Sound magnitude 8.4 earthquake was one of the largest ever on the North American Continent. These slides show geological changes, the effects of four major landslides triggered by the event, tsunami damage, and other damage to structures, transportation systems, and utilities.

Great Chile Earthquake of May 22, 1960 Anniversary Edition

This set documents the largest earthquake ever recorded, a magnitude 9.5 earthquake in southern Chile. This event ravaged southern Chile and generated a series of seismic sea waves (tsunami) that damaged not only Chile, but Hawaii and Japan and were observed throughout the Pacific.

Great Hanshin-Awaji (Kobe) Earthquake, January 17, 1995

The worst damage from this 6.9 magnitude earthquake occurred along a previously undetected fault, where many businesses and residences were located. This set shows damage in the downtown region and along the waterfront.

Hawaii Volcanism: Impact on the Environment

While not generally life-threatening, Hawaiian lava flows are highly destructive to populated and cultivated areas. This set depicts the impact on communities, vegetation, marine life, roads, and coastlines. It also shows the benefits including geothermal power, increased land area, and research opportunities.

Hawaii Volcanism: Lava Forms

Over the last several million years, the Hawaiian Islands were built of successive lava flows. These are the most recent additions to a long line of volcanoes trailing to the northwest. This set includes very colorful images of lava fountains, lakes, cascades, flows, spatter, and lava entry to the sea from recent eruptions.

Heinrich Events

25 slides show photos of icebergs, iceberg-rafted debris in marine sediment cores, and laboratory work on sediment cores. Graphics and discussion of Heinrich events, their causes, and their climatic significance are included.

Hokkaido Nansei-Oki Tsunami, July 12, 1993

Minutes after a magnitude 7.8 earthquake in the Sea of Japan, one of the largest tsunamis in Japan's history engulfed the coastline of Okushiri Island and the central west coast of Hokkaido. This set shows damage to ships, dwellings, and businesses, and clocks stopped by the tsunami.

Izmit, Turkey Earthquake, August 17, 1999: Coastal Effects

At 3:02 a.m. local time, a magnitude 7.4 earthquake occurred near the Izmit Bay, Marmara Sea, Turkey. The images show slope failure, subsidence, slumping, and liquefaction. The resulting tsunami wreaked havoc on waterfront properties.

Landers and Big Bear, California Earthquakes, June 28, 1992

The magnitude 7.6 earthquake near Landers, California was closely followed by a magnitude 6.7 near Big Bear. The two quakes were separated by 3 hours in time, 17 miles in distance, and 7,000 feet in elevation. This set depicts the terrain differences, structural damage, liquefaction, faulting, and resultant landslides.

Landslides, Set 1

The slopes above streams and rivers are subjected to processes that cause them to recede from the channel. These processes, collectively called mass wasting, are classified according to speed of movement and type of materials transported. This set depicts diverse types of mass wasting.

Landslides, Set 2

Expanding on the topics in Set 1, this set includes rockfalls, rock avalanches, mudflows, debris flows, slumps, creep, and sinkholes. Photos are from the western U.S., Puerto Rico, and Peru.

Loma Prieta Earthquake, Part 1

On October 17, 1989, a 7.1 magnitude earthquake occurred near Loma Prieta in the Santa Cruz Mountains. This set depicts earth cracks and structural damage in the more rural areas affected by the quake including Boulder Creek, Aptos, Los Gatos, San Jose, Scott's Valley, and Watsonville.

Loma Prieta Earthquake, Part 2

This set focuses on the effects of the earthquake (also known as the "San Francisco World Series Earthquake") in San Francisco and Oakland. It highlights the damage in the Marina District of San Francisco, Market Street, the San Francisco-Oakland Bay Bridge, and the Nimitz Freeway.

Low-Latitude Ice Cores

Photos of cores extracted from mountain ice caps in Peru and China. Images include: 3-D relief maps of the Andes and Himalayas; photos of fieldwork on the Quelccaya and Dunde ice caps; the core extraction process; and graphics depicting annual layering of ice, geochemical analyses, and climatic interpretation of ice core data.

Major Tsunamis of 1992 - Nicaragua and Indonesia

This set shows damage from the September, 1992 tsunami (waves 8-15 meters high) that struck Nicaragua's Pacific coast (6 slides) and the December, 1992 tsunami in the Flores region of Indonesia (14 slides).

Mount Pinatubo, Philippines: June 1991 Eruptions

On June 15, after two months of increasing activity following 635 years of quiet, Mount Pinatubo erupted cataclysmically. This set shows the early stages of the eruption phase, the eruption, and aftermath. Subsequent calamities caused by the ash, pyroclastic flows, mudflows, and flooding are depicted.

Mount Pinatubo Revisited:
A Study of Lahar Erosion

The 5 to 7 km^3 of material deposited in the 1991 eruption of Mount Pinatubo continues to threaten structures and lives in the form of debris flows (lahars) during heavy rainstorms. This set shows how the disaster that began at Pinatubo in 1991 continues to threaten the population in the area.

Northridge, California Earthquake, January 17, 1994, Set 1

On January 17, 1994, a magnitude 6.8 earthquake near downtown Los Angeles caused extensive damage in the San Fernando and Simi Valleys, and in the northern part of the Los Angeles Basin. This set shows damage to structures in Northridge.

Northridge, California Earthquake, January 17, 1994, Set 2

The January 1994 magnitude 6.8 earthquake near Los Angeles took 57 lives and caused $10 billion in property damage. This set includes damaged structures in communities including Sylmar, Fillmore, Granada Hills, Reseda, Van Nuys, Sherman Oaks, Chatsworth, Santa Monica, and Los Angeles.

Packrat Middens

Middens are deposits of plant material collected by packrats in caves in the arid SW United States. Middens are often preserved for thousands of years and can be used to reconstruct past vegetation and climate in the area of the midden deposit. 26 slides include photos of middens and the arid landscapes in which they are found, plus illustrations of sample analysis and reconstructions of vegetation and climate history.

Papua New Guinea Tsunami, July 17, 1998

On the evening of July 17, 1998, a magnitude 7.1 earthquake occurred near the northwest coast of Papua New Guinea 850 km northwest of Port Moresby. This set depicts damage from three catastrophic tsunamis following the earthquake that devastated several villages on the north coast.

Polar Ice Cores

This set of 37 images provides an overview of the long cores extracted from the Greenland and Antarctic Ice Sheets at Summit and Vostok. Core drilling and processing are presented in considerable detail and are followed by graphics highlighting important data sets and climatic interpretations.

Relief Globe Slide Set - Revised February 2000

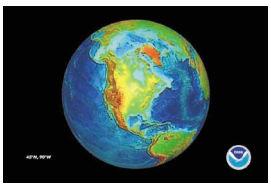

This updated, computer-generated set of 20 slides contains 14 global views of the Earth in full-color, shaded-relief, showing land and undersea topography. Also included are a Mercator projection view of the Earth, as well as displays of crustal plates and their relation to world seismic activity.

Rock Varnish

22 images in this set include aerial photographs of the Death Valley region, photomicrographs of various rock varnish layers, and an explaination of the climatic contexts in which these layers are formed.

San Fernando Valley, California Earthquakes

This set compares damage from the San Fernando (1971) and Northridge (1994) earthquakes. These two events, separated by 10 miles and 23 years, disproved the notion that once an earthquake has occurred, an area is safe from future earthquakes.

Seismic Creep

Seismic creep is the constant or periodic movement on a fault as contrasted with the sudden rupture associated with an earthquake. This set contains examples of creep from Hollister and Hayward, California. Several of the slides are split images of a location, comparing fault movement over the years.

Shikotan, Kuril Islands Earthquake, October 4, 1994, Set 1

This set shows damage from the magnitude 8.1 earthquake in the southern Kurils. Images include a newly-created landslide formation, ground cracks, structural damage, and effects of tsunami runup on Shikotan Island. A scientific overview of this event, written by a member of the international study team, is included.

Shikotan, Kuril Islands Earthquake and Tsunami, October 4, 1994, Set 2

This second set depicts much of the tsunami damage that occurred at Kuzhno-Kurilsk and Kunsashir Island. Tsunami heights ranged from 2.5-3.0 m. In the older part of town (fronted by a gentle beach) all houses were damaged by the wave that penetrated 200-500 m inland.

Tree Rings

Photos depicting dendrochronological techniques, including tree coring in the field, sample preparation, cross-dating, standardization, and chronology building. Photos and graphics of tree physiology as well as climatic interpretations derived from tree-ring data.

Tropical Cyclones - 1995 Atlantic Hurricanes

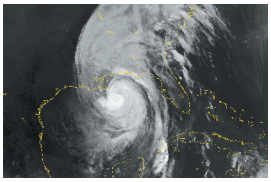

During the 1995 hurricane season, eleven tropical cyclones reached hurricane status, nearly double the average. A set of 22 slides with each slide displaying a storm in either visible or infrared wavelengths. Winds from Hurricane Opal reached 130 kt. **All Tropical Cyclone sets include descriptions of storm damage and maps of the storm tracks.** B&W

Tropical Cyclones - 1995 NW Pacific Typhoons

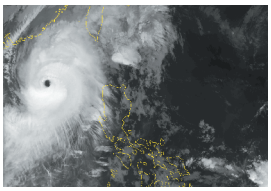

Set of 23 slides showing 1995's 12 typhoons. The DMSP satellite's unique imagery supports study of the structure, magnitude, and location of storms. Each slide displays a storm in either visible or infrared wavelengths. Winds from Typhoon Angela exceeded 155 kt. B&W

Tropical Cyclones - 1996 Indian Ocean & SW Pacific

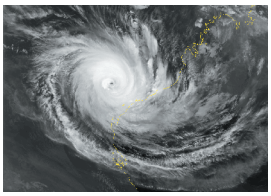

40 slides show each of the 20 typhoon-class cyclones in thermal-infrared and visible wavelengths. Only one of these cyclones occurred north of the equator. Winds from Cyclones Bonita and Itelle exceeded 140 kt. B&W

Tropical Cyclones - 1996 NE Pacific & Atlantic Hurricanes

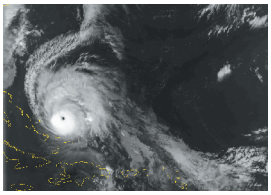

26 slides from 13 hurricanes show each hurricane in thermal-infrared and visible wavelengths. Five storms occurred in the Northeast Pacific and 8 occurred in the North Atlantic. Winds from Hurricane Edouard reached 126 kt. B&W

Tropical Cyclones - 1996 NW Pacific Typhoons

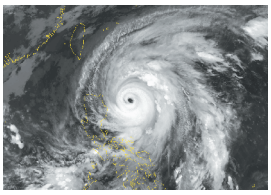

42 slides show each of the 21 typhoons in thermal-infrared and visible wavelengths. Typhoon Dale, the most intense tropical storm of the year with winds exceeding 150 kt, is included in this set. B&W

Tropical Cyclones - 1997 Indian Ocean & SW Pacific

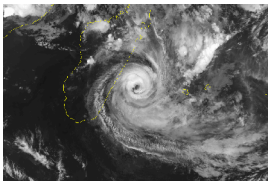

40 images comprise this set of 20 storms of severe cyclone strength in the Indian and Southwest Pacific Oceans which occurred between January 2, 1997 and January 1, 1998. Each storm is displayed in thermal-infrared and visible wavelengths. Two cyclones, Poncho-Helinda and Gavin, had sustained winds of 128 kt. B&W

Tropical Cyclones - 1997 NE Pacific & Atlantic Hurricanes

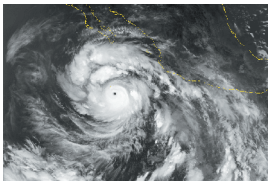

24 slides comprise this set of 12 Western Hemisphere hurricanes that occurred between July 5 and November 10, 1997. Hurricane Linda, estimated as the year's strongest hurricane in the eastern North Pacific Ocean with sustained winds reaching 160 kt, is included in this set. B&W

Tropical Cyclones - 1997 NW Pacific Typhoons

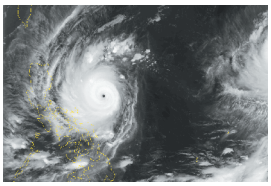

42 images comprise this slide set of 21 Northwest Pacific storms of typhoon strength that occurred between April 11 and December 21, 1997. Each storm is displayed in both thermal-infrared and visible wavelengths. Four typhoons, Ivan, Joan, Keith, and Paka all had sustained winds of 160 kt. B&W

Tropical Cyclones - 1998 Atlantic Hurricanes

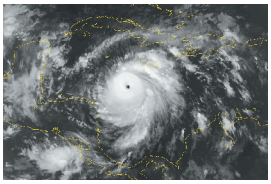

During 1998, 10 tropical storms reached hurricane strength in the Atlantic Ocean. 20 slides show hurricanes in both thermal-infrared and visible wavelengths. Hurricane Mitch had sustained winds of 168 kt and was responsible for over 9,000 deaths in Central America. B&W

Tropical Cyclones - 1998 Indian Ocean Cyclones

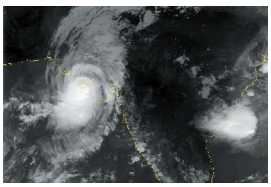

This set of 26 slides presents images of 13 tropical storms in thermal-infrared and visible wavelength. Cyclone 03A, the most intense cyclone to strike India in 25 years, caused the dislocation of over 15,000 people by damaging or destroying thousands of homes. B&W

Tropical Cyclones - 1998 NE Pacific Hurricanes

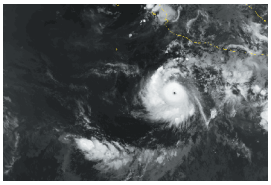

18 images comprise this set of 9 tropical storms with each displayed in thermal-infrared and visible wavelength. Hurricane Howard, estimated to be the strongest 1998 hurricane in the NE Pacific reached a maximum wind speed of 130 kt. B&W

Tropical Cyclones - 1998 NW Pacific Typhoons

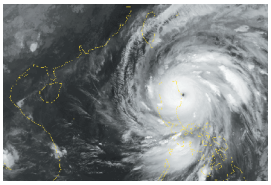

This slide set shows satellite views of 9 NW Pacific Typhoons. 18 slides show each hurricane in both thermal-infrared and visible wavelengths. Winds from Typhoon Zeb reached 155 kt. B&W

Tropical Cyclones - 1998 Southwest Pacific

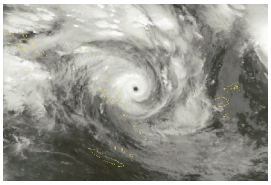

16 images show 8 cyclones in both thermal-infrared and visible wavelengths. Cyclone Ron produced sustained winds of 155 kt. B&W

Tsunamis – General

Tsunami, a Japanese word meaning "harbor wave", is a series of water waves generated by sudden displacement of the ocean or other body of water. This set depicts advancing waves, harbor damage, and structural damage from seven tsunami events in the Pacific region since 1946, including before-and-after views of Scotch Cap Lighthouse (Aleutian Islands). B&W/Color

Volcanic Rocks and Features

Volcanoes are one of the more dramatic manifestations of the dynamic nature of Earth. The rocks and features formed in an eruption reveal a great deal about the process. Pictures show lava types, ash, cinders, bombs, necks, dikes, and sills.

Volcanoes in Eruption, Set 1

This slide set depicts explosive eruptions, lava fountains and flows, steam eruptions, and fissure eruptions from 19 volcanoes in 13 countries. Volcano types represented include: strato, cinder cone, complex, fissure vent, lava dome, shield, and island-forming. B&W/Color

Volcanoes in Eruption, Set 2

This set depicts ash clouds, fire fountains, lava flows, spatter cones, glowing avalanches, and steam eruptions from 18 volcanoes in 13 countries. Volcano types include: strato, cinder cone, basaltic shield, complex, and island forming. B&W/Color

Unless otherwise noted, each set contains 20 color slides.

ORDERING INFORMATION

U.S. Department of Commerce regulations require **PREPAYMENT** on all orders, with the exception of those from U.S. governmental agencies. Due to recent legislation, prices are subject to change without notice. **Please check the NOAA National Data Centers' Online Store or call for price verification.**

Make checks or money orders payable to NOAA National Data Centers. **Do not send cash.** All foreign payments must be in U.S. dollars, drawn on a U.S. bank. We accept American Express, MasterCard, VISA, or Discover by telephone, letter, fax, or order form. Please include a credit card account number, expiration date, telephone number, and the cardholder's name and signature with the order.

These slide sets may be ordered online with payment by American Express, MasterCard, VISA, or Discover. Additional information, points of contact, and the NOAA National Data Centers' Online Store can be accessed through the digital version of this flier located at URL:

http://www.ngdc.noaa.gov/products/ngdc_slides.html

Your World Wide Web browser must support the SSL security protocol to place an online order.

All data listed in this flier are available from:

NOAA National Data Centers
325 Broadway, E/GC4, Dept A05
Boulder, CO 80305-3328
USA

Phone: (303) 497-6826
FAX: (303) 497-6513
Voice/TDD: (303) 497-6958
Email: info@ngdc.noaa.gov
WEB: http://www.ngdc.noaa.gov/

Data contributors and academic researchers should call for information about obtaining data through cooperative exchanges.